Available online at www.sciencedirect.com
SCIENCE DIRECT®
Microelectronic Engineering 83 (2006) 126–129
MICROELECTRONIC ENGINEERING
www.elsevier.com/locate/mee

Raman scattering characterization on SiC

Hiroshi Harima *

Department of Electronics and Information Science, Kyoto Institute of Technology, Matsugasaki, Sakyo-ku, Kyoto 606-8585, Japan

Available online 18 November 2005

Abstract

Raman scattering is a powerful non-contact and non-destructive characterization tool for SiC polytypes for both the lattice and electronic properties. Here, I will briefly review two recent Raman experiments on SiC; metal/SiC interface reactions probed by visible lasers and ion-implantation damages probed by deep UV lasers. These studies utilize the opposite aspects of the probe laser, i.e. deep and shallow penetration depth into SiC.

PACS: 78.30.-j; 63.20.-e; 73.40.Cg; 61.72.Ww

Keywords: Raman scattering; SiC; Phonon; Interface; Ion-implantation; UV laser

1. Introduction

Raman scattering efficiency of SiC is relatively high because of strong covalency in the chemical bonding, and we can easily extract various useful information on SiC by Raman scattering such as polytype, disorder or damage, lattice strain, temperature, impurities, free carrier density and mobility [1,2]. Here, I will briefly introduce two recent experiments to study metal/SiC interface reactions using visible lasers, and ion-implantation-induced damages using deep UV lasers. They are related to metallization and doping techniques, respectively, and may provide convenient tools in SiC-device fabrication processes.

2. Effective penetration depth of probe laser

SiC has relatively low absorption coefficients in the visible region, and gives large penetration depth for Raman probe lasers. In the case of back scattering geometry, since the scattered photons are absorbed by the material on the way back, the effective penetration depth δ is roughly evaluated by $\delta = 1/(2\alpha)$, where α is the absorption coefficient. If we consider here only 6H-SiC ($E_g = 3.0$ eV) and 4H-SiC (3.2 eV), and use reported absorption coefficients for high quality samples [3,4], we obtain as a typical value $\delta = 2$ mm for visible lasers at wavelength ~500 nm (2.5 eV in photon energy). However, the depth rapidly decreases when UV lasers are employed as shown schematically in Fig. 1; $\delta = 50$–100 μm for 364 nm and $\delta = 50$–100 nm for 244 nm excitation. (Some commercial laser wavelengths are considered as example.) It should be noted that 4H-SiC gives roughly two times greater penetration depth than 6H-SiC at 350–250 nm (3.5–5 eV), because of the difference in band gap energy. We can utilize both merits, the long and short penetration depths for visible and UV lasers, respectively, to Raman characterizations as described below.

3. Metal/SiC interface reaction

Conventional methods for investigating metal/SiC interface reaction such as Auger electron spectroscopy (AES), secondary-ion mass spectrometry (SIMS) and Rutherford back scattering (RBS) are all destructive characterization and give elemental abundance as a function of depth. While it is often difficult to specify the reaction products by these studies, Raman microprobe may provide such information non-destructively with a spatial resolution of ~1 μm. Furthermore, when visible lasers are used, we can probe the metal/SiC interface from the substrate side

* Tel./fax: +81 75 724 7421.
E-mail address: harima@dj.kit.ac.jp.

0167-9317/$ - see front matter © 2005 Published by Elsevier B.V.
doi:10.1016/j.mee.2005.10.037

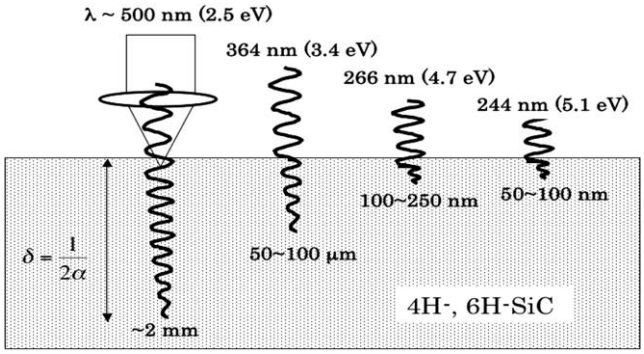

Fig. 1. Effective penetration depth for different excitation wavelengths. The penetration depth is not much influenced by the setup; microscopic or macroscopic Raman scattering.

through a thick SiC wafer using a long laser penetration depth.

Fig. 2 shows such an example [5]: the Raman spectra were observed from both sides of the specimen as illustrated in the inset; the probe laser (515 nm) was incident from the Ni-electrode side (a) or incident from the opposite side through the SiC wafer (b). The samples were prepared by depositing a Ni layer (200 nm thick) on the carbon face of a both-side polished *n*-type 6H-SiC wafer (0.4 mm thick), followed by annealing in Ar atmosphere at 500–1100 °C. In Fig. 2(b), the sharp intense signals observed in all spectra at 145 and 149 cm^{-1} (asterisk) are E_2-phonon modes from the SiC wafer [1]. Absence of these signals in Fig. 2(a) means that the probe laser did not reach the wafer region. By referring to reported Raman data [6,7], the other signals derived from three kinds of nickel silicides; Ni_2Si (100, 140 cm^{-1}), NiSi (190, 215 cm^{-1}) and $NiSi_2$ (260, 310, 370 cm^{-1}). When observed from the Ni side (Fig. 2(a)), the nickel silicide signals appeared at above 900 °C, while they appeared at above 500 °C when observed from the wafer side (Fig. 2(b)).

Current–voltage (*I–V*) characteristics plotted in Fig. 3 shows that ohmic contact is obtained by annealing at above 900 °C. This correlates well with the Raman spectral

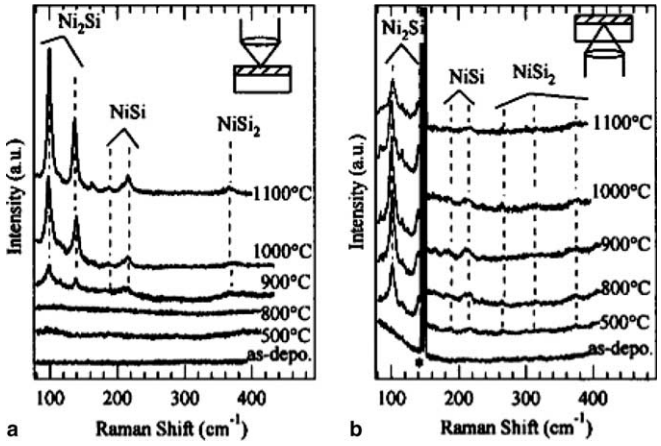

Fig. 2. Raman spectra observed from Ni side (a) and from 6H-SiC wafer side (b) [5].

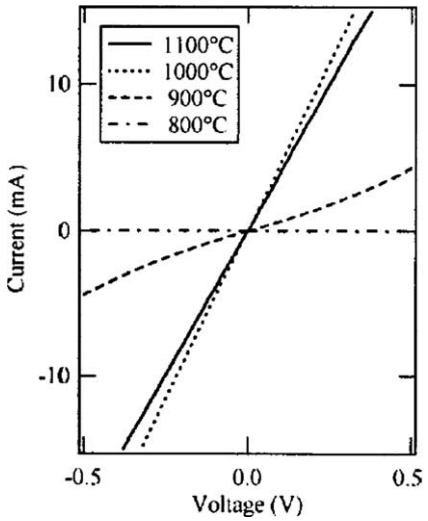

Fig. 3. Variation of *I–V* characteristics with annealing temperature [5].

features: formation of nickel silicides at 500–800 °C in the interface region (Fig. 2(b)) is not a key factor, but the formation of nickel silicide (especially Ni_2Si) throughout the Ni layer (Fig. 2(a)) is more important. This was confirmed by AES, and agrees with a previous experiment by RBS and AES [8]. Carbon atoms that did not react with Ni may form carbon clusters at the interface. Kurimoto et al. [5] revealed by Raman scattering that graphite nano-particles of 5–10 nm in size were distributed throughout the Ni layer when annealed at 1000–1100 K [5].

4. Ion-implantation-induced damage

Ion-implantation is an important doping technique in SiC. As a typical case, nitrogen or phosphorous ions are implanted at multiple implantation energies up to ~300 keV to form a box-type impurity distribution to a depth of ~300 nm in SiC. Since deep UV lasers with wavelength

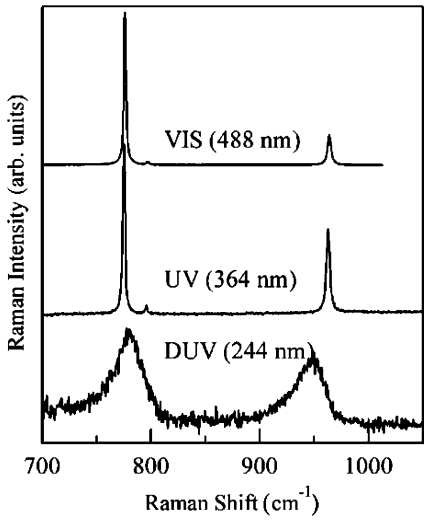

Fig. 4. Raman spectra of as-implanted sample observed at different probe lasers [9].

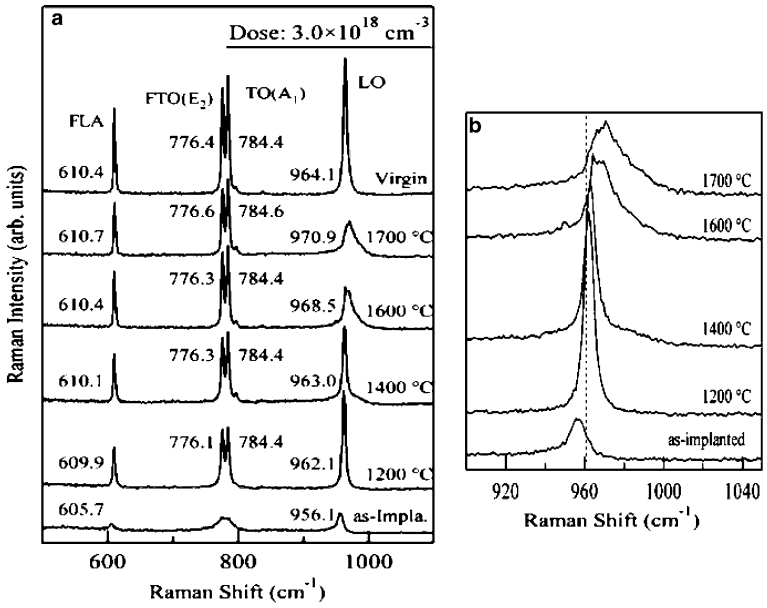

Fig. 5. Raman spectra observed by 244 nm excitation for samples annealed at 1200–1700 °C (a) and the LO phonon region expanded (b) [9].

~250 nm (5 eV) provide shallow penetration depth to mach this projection range, they are ideal excitation sources to probe the implanted region without interference from the underlying layer.

Nakashima et al. [9] reported quite recently a precise Raman study on P^+-implanted 4H-SiC using a deep UV (DUV) laser at 244 nm (second harmonic of an Ar^+-laser at 488 nm) [9]. They used *p*-type epitaxial layers (hole concentration $5 \times 10^{15}\,cm^{-3}$) grown on (0001) 4H-SiC substrates, and ion-implanted to make a box-profile impurity distribution with depth 300 nm. Dependence of the effective penetration depth on the probe-laser wavelength is well demonstrated in Fig. 4. Here, the sample was implanted at room temperature and post-annealed at 1200 °C for 30 min. The DUV spectrum shows broad TO and LO bands (around 780 and 960 cm^{-1}, respectively) deriving from the amorphized region induced by the implantation damage. The visible (488 nm) and UV (364 nm) spectra show, on the other hand, only sharp bands because the signals are dominated by those from the underlying layer not implanted. This result clearly shows that the probed region is shallower than the ion-projected range of 300 nm.

Fig. 5(a) shows Raman spectra probed by 244 nm excitation. Here, the samples were P^+-implanted at 500 °C to reduce the damage (hot implantation), and subsequently annealed at various temperatures in 1200–1700 °C. Even the as-implanted sample (bottom) is not completely amorphized because of hot implantation. As the annealing temperature is raised, the TO bands become sharper and more intense, to be well separated into two components at 776.4 and 784.4 cm^{-1} just like the virgin crystal (top). The LO phonon region is expanded in Fig. 5(b). For 1200 °C annealing, the LO band is sharp and peaked at the same frequency as the virgin crystal (dotted line). However, the peak shifts to higher frequency and broadens asymmetrically at higher annealing temperatures. This is a typical behavior of LO-phonon-plasmon-coupled mode (LOPC mode), so that we can deduce the free carrier density *n* by analyzing the spectral line shape [1]. Nakashima et al. [9] obtained $n = 1.5 \times 10^{18}\,cm^{-3}$ for the 1700 °C-annealed sample, and evaluated the electrical activity of impurity as 50% [9]. The sharp LO phonon profiles for the 1200–1400 °C-annealed samples were attributed to incomplete recovery in crystallinity, which generated plenty of deep level defects acting as traps of free carriers.

5. Conclusion

Recently, commercial deep UV lasers at wavelength 250–300 nm (4–5 eV) have become familiar along with the advancement of related optical components and detection systems. In Raman scattering of SiC, we can now select a suitable probe depth in the range from millimeter to 100 nm or less. This choice will further increase the potential of Raman scattering characterization in SiC materials and their devices.

References

[1] (a) S. Nakashima, H. Harima, in: W.J. Choyke, H. Matsunami, G. Pensl (Eds.), Silicon Carbide – A Review of Fundamental Questions and Application to Current Device Technology, Akademie Verlag, Berlin, 1997, p. 39;
(b) S. Nakashima, H. Harima, Phys. Stat. Solidi A 162 (1997) 39.
[2] S. Nakashima, H. Harima, in: W.J. Choyke, H. Matsunami, G. Pensl (Eds.), Silicon Carbide-Recent Major Advances, Springer, Berlin, 2004, p. 585.
[3] S. Logothetidis, J. Petalas, J. Appl. Phys. 80 (1996) 1768.
[4] S. Zollner, J.G. Chen, E. Duda, T. Wetteroth, S.R. Wilson, J.N. Hilfiker, J. Appl. Phys. 85 (1999) 8353.
[5] E. Kurimoto, H. Harima, T. Toda, M. Sawada, M. Iwami, S. Nakashima, J. Appl. Phys. 91 (2002) 10215.

[6] P.S. Lee, D. Mangelinck, K.L. Pey, Z.X. Shen, J. Ding, T. Osipowicz, S. See, Electrochem. Solid State Lett. 3 (2000) 153.
[7] F. Li, N. Lustig, P. Klosowski, J.S. Lannin, Phys. Rev. B 41 (1990) 10210.
[8] J. Crofton, L.M. Porter, J.M. Willams, Phys. Status Solidi 202 (1997) 581.
[9] S. Nakashima, T. Mitani, J. Senzaki, H. Okumura, T. Yamamoto, J. Appl. Phys. 97 (2005) 123507.